Title: Adsorption of Ni(II) on spent coffee and coffee husk based activated carbon

Authors: Mónica Hernández Rodríguez, Jan Yperman, Robert Carleer, Jens Maggen, Dessalegn Daddi, Grazyna Gryglewicz, Bart Van der Bruggen, José Falcón Hernández, Alexis Otero Calvis

PII: S2213-3437(17)30684-X
DOI: https://doi.org/10.1016/j.jece.2017.12.045
Reference: JECE 2092

To appear in:

Received date: 28-9-2017
Revised date: 7-12-2017
Accepted date: 20-12-2017

Please cite this article as: Mónica Hernández Rodríguez, Jan Yperman, Robert Carleer, Jens Maggen, Dessalegn Daddi, Grazyna Gryglewicz, Bart Van der Bruggen, José Falcón Hernández, Alexis Otero Calvis, Adsorption of Ni(II) on spent coffee and coffee husk based activated carbon, Journal of Environmental Chemical Engineering https://doi.org/10.1016/j.jece.2017.12.045

Adsorption of Ni(II) on spent coffee and coffee husk based activated carbon

Mónica Hernández Rodríguez[a,d], Jan Yperman[b*], Robert Carleer[b], Jens Maggen[b], Dessalegn Daddi[c], Grazyna Gryglewicz[e], Bart Van der Bruggen[f], José Falcón Hernández[d], Alexis Otero Calvis[a]

[a]*Mineral and Metallurgic Institute (ISMM), Moa, Holguín, Cuba*

[b]*Research group of Applied and Analytical Chemistry, Hasselt University, Agoralaan building D, 3590-Diepenbeek, Belgium*

[c]*Department of Environmental Health Sciences & Technology, Jimma University, Ethiopia*

[d]*Faculty of Chemical Engineering, Universidad de Oriente, Santiago de Cuba, Cuba*

[e]*Department of Polymer and Carbonaceous Material, Faculty of Chemistry, Wroclaw University of Technology, Gdanska 7/9, 50-344 Wroclaw, Poland*

[f]*Process Engineering for Sustainable Systems Section, Department of Chemical Engineering, University of Leuven, Celestijnenlaan 200F, 3001 Leuven, Belgium; and Faculty of Engineering and the Built Environment, Tshwane University of Technology, Private Bag X680, Pretoria 0001, South Africa.*
*Corresponding author. Tel: +32(0)11 268320; Fax: +32(0)11 268301.

E-mail address: jan.yperman@uhasselt.be

Abstract

Adsorption of Ni(II) on low cost activated carbon (AC) from spent coffee (SAC) and coffee husk (HAC) has been studied. Porous textures of adsorbents were characterized by N_2 and CO_2 sorption measurements. Batch adsorption experiments were performed as a function of adsorbent dose, Ni(II)-concentration and pH. Adsorption of Ni(II) was evaluated using different adsorption isotherm models (Langmuir, Freundlich, Monolayer Model for Single-Compound Adsorption and Dubinin – Radushkevich) and thermodynamics and kinetics parameters were determined. Both adsorbents show high affinity for Ni(II), however both the surface area and the pore size of the ACs do not seem to be the determining factor in the adsorption process. These ACs are microporous in nature. In contrast, the higher oxygen amount associated to the mineral matter as K_2O and carbon functionalities corresponding with O–H in HAC are determining for the Ni-ion adsorption process and multi-ion anchorage mechanism. In addition, the exchange of potassium present in the ACs improves the Ni(II) adsorption process. Thermodynamics and kinetics evidence a fast and endothermic adsorption process. The maximum adsorption capacity using the Langmuir isotherm model was found to be 57.14 mg/g and 51.91 mg/g for HAC and SAC, respectively. The sorption efficiency was higher for HAC as adsorbent. At low concentrations of Ni(II) (30 mg/L) and higher temperatures (308-328 K), removals > 94% were measured for HAC, achieving safe discharge concentration values.

Keywords: Adsorption; Ni(II); spent coffee; activated carbon; coffee husk

1. Introduction

Nowadays the increase of environmental problems and concerns, caused by contaminations with heavy metals, have catalysed the search and development of technologies to treat polluted waters from different industries: metallurgic plants, electroplating, alloys and battery manufacturing [1, 2]. Additionally, heavy metal ions do not degrade, persist in the environment and tend to accumulate in living organisms. Due to their toxicity, the treatment of wastewater contaminated with these metals is a priority concern [3, 4].

Current technologies for the treatment of wastewater include coagulation/flocculation, precipitation, sedimentation or filtration, membrane processes, ion exchange, and adsorption using activated carbon (AC) [5, 6]. However, the cost of these methods hinders their application [7]. Additionally, at low concentration (1 - 100 mg/L) many of these treatments are rather cost-ineffective [8].

ACs are very effective in treating aqueous solutions containing low concentrations of metal ions [9-13]. Due to their high amount of micropores and mesopores, their large surface area [3], the variety of surface functional groups interacting with the heavy metal ions and even the possibility to increase the adsorption capacity by modifying with other functional groups or using additives [3, 14-16], these adsorbents are interesting candidates for wastewater treatment.

The agro-wastes receive much more attention as a cheap source for the production of ACs; its cost-effectiveness makes this alternative attractive particularly for small-scale industries [17-20]. Agricultural waste for AC production is mainly coming from shell and stones of the fruits [21]. However, waste resulting from the production of cereals like rice, coffee, maize and corn receives more and more attention. The preparation of AC from waste materials using pyrolysis offers economic and environmental advantages [22]. Several authors have produced ACs from coffee residues for the adsorption of organic pollutants [23-28]. Nevertheless, their use in the removal of toxic heavy metals [29-31] has been less studied. Also the contribution of ACs textural and chemical characteristics including mineral matter in the adsorption mechanism needs to be further assessed.

Nickel is a toxic metal. Mineral processing of this element leaves high levels of nickel ions in the aquatic environment [4]; around 45 mg/L is determined in the liquor waste from an acid leaching technology. In addition, nickel salts are known to be carcinogenic. According to the World Health Organization (WHO) general "safe" concentration values should be below 0.2 mg/L [32, 33].

The present research studies the adsorption of Ni(II) from an aqueous solution with similar concentrations to the liquor waste from an acid leaching technology, using a low cost activated carbon from spent coffee (SAC) and coffee husk (HAC). Adsorbent doses and solution pH are evaluated using batch adsorption tests. Langmuir, Freundlich, a Monolayer Model for Single-Compound Adsorption and Dubinin - Radushkevich models are used to describe the adsorption process. Thermodynamic and kinetic parameters are also evaluated. The characterization of the adsorbent materials include: pH at the point of zero charge (pH_{PZC}), Boehm titration, BET analysis, elemental analysis, X-ray photoelectron spectroscopy (XPS) and ATR-FTIR measurements, to understand surface properties and available functional groups involved in the adsorption mechanism.

2. Materials and Methods

2.1. Chemicals

All reagents used were of analytical grade and purchased from Merck. Metal solutions were prepared by dissolving $NiSO_4 \cdot 7H_2O$ in Milli-Q water to obtain a stock solution of 5000 mg/L. All other solutions were prepared by diluting this stock solution. The pH of the solution was adjusted with 0.1 N NaOH or 0.1 N HCl solutions. The concentration of nickel ions was determined using an inductively coupled plasma spectrophotometer (Perkin Elmer Optima 3000 DV ICP-AES device with an axial plasma configuration).

2.2. Raw materials, preparation and characterization of adsorbents

Spent coffee and coffee husk were acquired from Jimma, Ethiopia. Activated carbons have been prepared from the above materials. Samples were first pyrolyzed in an oxygen-free atmosphere (N_2) in a lab-scale reactor. For each experiment, a known amount of sample is introduced into the reactor. After the reactor is sealed and placed under a stream of nitrogen (2 x 70 mL/min) the reactor is heated with a rate of 10°C/min to 500°C and then hold isothermal for 1 hour for a complete pyrolysis. The sample is continuously kept in motion by an Archimedes screw in order to achieve a uniform heat distribution. The reactor is heated up with a tailored heating mantle, and the temperature is checked using a thermocouple located inside the reactor [34]. During the thermal treatment, the sample is subjected to a thermal cracking and volatilization. The formed gases leave the reactor and are collected in a condensation unit. The condensed fraction is pyrolytic oil. The formed biochar remains in the reactor and the non-condensable gases leave the system. The biochar is activated in a second step.

For activation, the biochar was the introduced in a horizontal quartz reactor and fixed with two quartz wool plugs. The biochar was heated up under a N_2 atmosphere to 800°C at 20°C/min. At 800°C the

atmosphere was switched from nitrogen to water vapour (10 mL) to complete the activation process for 30 min.

The pH at zero charge (pH_{PZC}) and the amount of surface functional groups were determined by an acid–base titration procedure. The procedure for the pH_{PZC} determination is described elsewhere [35, 36]. In brief, 50 mL of a 0.01 N NaCl solution was adjusted between pH 2 and 12 with the addition of a solution of 0.01 N HCl or 0.01 N NaOH in different flasks. Then, 0.15 g of activated carbon sample was added to each flask and the resulting solution was shaken for 48 h. The final pH was measured. The pH_{PZC} value is the point where the curve pH_{final} versus $pH_{initial}$ crosses the line $pH_{initial} = pH_{final}$.

The number of total acidic or basic surface groups was determined according to the Boehm titration method. The adsorbent (1.0 g) was added to 50 mL of the following solutions: NaOH (0.05 N), Na_2CO_3 (0.05 N) and $NaHCO_3$ (0.05 N). The flasks were sealed and shaken for 24 h. Subsequently, 10 mL of each filtrate was pipetted; excess of base or acid was titrated with HCl (0.05 N) to a pH of around 7. The method is based on the theory that NaOH neutralizes carboxyl, lactone and phenolic groups, Na_2CO_3, carboxyl and lactone, while $NaHCO_3$ only neutralizes carboxyl groups [37-39].

Porous texture analysis has been carried out by N_2 and CO_2 adsorption at 77 and 273 K, respectively, in an Autosorb iQ apparatus (Quantachrome Instruments). The samples were outgassed overnight at 300ºC before N_2 adsorption and for 5 h at 300ºC before CO_2 adsorption under high vacuum. The specific surface area (S_{BET}) was calculated from the N_2 sorption isotherm data using the BET (Brunauer, Emmett and Teller) method. The amount of nitrogen adsorbed at the relative pressure of p/p_0=0.98 was used to determine the total pore volume (V_T). The N_2 isotherms in the p/p_0 range from 0 to 0.96 reflect that the adsorption takes place in the mesopores (pores with a width of 2-50 nm) and in the micropores larger than 0.7 nm. The micropore volume ($V_{DR,N2}$) and the average micropore size ($L_{0,N2}$) were estimated by applying the Dubinin-Radushkevitch and Stoeckli equations to data collected at low pressures (p/p_0<0.015) [40]. The Quenched-Solid Density Functional Theory (QSDFT) analysis [41] was applied to the N_2 adsorption isotherms to determine pore size distribution (PSD).

The CO_2 isotherms at 273 K and low relative pressure (p/p_0<0.1) are assumed to correspond to the adsorption taking place in the narrow micropores in the range of 0.4-0.8 nm (ultramicropores). These isotherms were used to calculate the ultramicropore volume ($V_{DR,CO2}$) and ultramicropore size ($L_{0,CO2}$) by means of the Dubinin-Radushkevitch and Stoeckli equations, respectively [40]. Assuming the presence of slit-shaped ultramicropores, the surface of their walls was determined from the following equation: S_{CO2} (m^2/g)=2000 $V_{DR,CO2}/L_{0,CO2}$ [42]. The PSD was also calculated from the CO_2 isotherm data by applying the Non-Local Density Functional Theory (NLDFT) [43] in order to characterize ultramicropores.

The elemental analysis of C, H, N and S was performed using a Vario MICRO cube analyser, and the oxygen content was directly measured using a Carlo Erba EA 1108 Elemental Analyzer with BBOT (2,5-bis(5-tert-butyl-benzoxazol-2-yl) thiophene with formula $C_{26}H_{26}N_2O_2S$) as standard for calibration. The surface elemental compositions of ACs were determined by X-ray photoelectron spectroscopy (XPS) using a PHI 5000 VersaProbe spectrometer. The XPS spectrum was calibrated with respect to the C1s signal at 284.5 eV. Curve fitting was performed by an iterative least-squares algorithm (CasaXPS software) using a Gaussian-Lorentzian (70/30) peak shape and applying the Shirley background correction.

ATR-FTIR measurements were performed to assess the functional groups involved in the adsorption mechanism. The dried samples were directly measured in the wavenumber range from 4000 to 600 cm^{-1} with a resolution of 4 cm^{-1} using a Bruker Vertex 70 equipped with a DTGS detector (32 scans) using a diamond ATR crystal.

2.3. Effect of adsorbent doses and solution pH

The effect of adsorbent doses and solution pH was studied using batch adsorption experiments at 25±1°C in an erlenmeyer of 250 mL. The amount of adsorbent, between 20–120 mg, was added to the erlenmeyer containing 100 mL of 45 mg/L Ni(II). The pH value was adjusted to 6 using 0.1 N of NaOH or HCl solution. The erlenmeyer was sealed and shaken during 24 h. After agitation, the adsorbent was removed using a cellulose Ø 150 mm filtration paper. From this, 10 mL was taken to determine the concentration

of Ni(II). At the optimal adsorbent doses, the effect of solution pH was examined in the same conditions but varying the pH within the range of 2–8.

2.4. Adsorption isotherms

At the optimal adsorbent dose and solution pH, adsorption isotherm experiments were carried out at 25±1°C in an erlenmeyer of 250 mL. The adsorbent was added to 100 mL Ni(II) solution (30, 40, 60, 80, 100 and 120 mg/L). All experiments were performed at 24 h contact time. After each experiment, the solution was filtered and the concentration of Ni(II) was determined.

The amount of Ni(II) adsorbed qe (mg/g) at equilibrium, was calculated using the following equation:

$$q_e = \frac{C_0 - C_e}{m} \times V \quad (1)$$

where C_0 and C_e are the initial and equilibrium concentration of Ni(II), respectively (in mg/L), V is the volume of the solution (L) and *m* is the weight of the adsorbent used (g).

The removal percentage of adsorbed heavy metal was estimated by:

$$R_{emoval}(\%) = \frac{C_o - C_e}{C_0} \times 100 \quad (2)$$

Freundlich, Langmuir, Monolayer Model for Single-Compound Adsorption and Dubinin - Radushkevich models were fitted to the adsorption isotherm data for equilibrium description. The Freundlich isotherm is an empirical model and can be applied to multilayer adsorption, with non-uniform distribution of adsorption, heat and affinities over the heterogeneous surface [44, 45]. In its linear form it is given by:

$$\log q_e = \log K_F + \frac{1}{n} \log C_e \quad (3)$$

where K_F is related with the adsorption capacity ($mg^{1-1/n}L^{1/n}g^{-1}$) and *n* is related to the adsorption intensity, also known as the heterogeneity factor [44].

The Langmuir isotherm is based on a theoretical model where the intermolecular forces decrease rapidly with the distance and assumes a monolayer adsorption over an energetically homogeneous adsorbent surface containing a finite number of adsorption sites. It does not take interactions between adsorbed molecules into account [46, 47]. It can be represented by the following linear equation:

$$\frac{1}{q_e} = \frac{1}{q_m} + \left(\frac{1}{K_L q_m}\right) \frac{1}{C_e} \quad (4)$$

where q_m and K_L are constants related to the maximum adsorption capacity (mg/g) and the adsorption energy (L/mg), respectively. Hereby, a dimensionless constant, known as the separation factor (R_L) [48] can be defined by:

$$R_L = \frac{1}{1 + K_L C_0} \quad (5)$$

The R_L value indicates the nature of adsorption to be either unfavourable (R_L>1), linear (R_L=1), favourable (0<R_L<1) or irreversible (R_L=0) [8].

Nevertheless, Langmuir model assumes that the adsorbed molecule or ion occupies one site of adsorption. In order to clarify the adsorption mechanism, the number of ions per site of adsorption can also be determined using a Monolayer Model for Single-Compound Adsorption (MM-SCA) developed by *Sellaoui et al.* [49, 50]. This model is based on the Hill isotherm, which assumes that the adsorption is a cooperative phenomenon. A determined number of molecules (nA) can be adsorbed onto one or several receptor sites (S). The mathematical model is expressed by the following equation [50]:

$$q_e = \frac{nN_m}{1 + \left(\frac{C_{e/2}}{C_e}\right)^n} \quad (6)$$

where $nN_m = Q_0$ is the monolayer adsorbed quantity obtained at saturation (mg/g), N_m is the density of receptor sites, *n* is the number of ions per site and $C_{e/2}$ is the concentration at half saturation (mg/L).

The Dubinin–Radushkevich (D–R) is an empirical model initially conceived for the adsorption of subcritical vapours onto micropore solids following a pore filling mechanism [45]. The approach was usually applied to distinguish the physical and chemical adsorption of metal ions [45, 51]. The linear model is given by:

$$\ln q_e = \ln q_s - K_D \varepsilon^2 \quad (7)$$

$$\varepsilon = RT\, ln\left(1 + \frac{1}{C_e}\right) \quad (8)$$

where q_s is the maximum sorption capacity of the adsorbent (mg/g), ε is the Polanyi sorption potential and K_D (mol^2/J^2) is a constant related to the mean energy of sorption per mole of adsorbate as it is transferred from the bulk solution to the surface of the solid. This energy E (kJ/mol) is determined by the following equation [45]:

$$E = \frac{1}{\sqrt{2\,K_D}} \quad (9)$$

The parameter E is used for estimating the type of adsorption. If this value is below 8 kJ/mol the adsorption type is related to physical adsorption, between 8 and 16 kJ/mol the adsorption is due to ion exchange, and above 16 kJ/mol the adsorption type is a stronger chemical adsorption [8, 52].

2.5. Reusability of activated carbons

After determining the best conditions for the adsorption process (adsorbent doses and solution pH), the desorption of loaded Ni ions onto ACs was carried out under a similar procedure (batch experiments at 25±1°C in an erlenmeyer of 250 mL, shaken during 24 h). A determined amount of AC-Ni was added to 100 mL of 0.1 N HCl solution. Then the adsorbent was separated and the residual concentration of Ni(II) ions was determined. The activated carbons were dried at 105±5°C and used in the next cycle of adsorption-desorption test. The removals and desorption effectiveness during three adsorption-desorption cycles were evaluated.

2.6. Thermodynamic and kinetic parameters

The free energy change ($\Delta G°$), enthalpy change ($\Delta H°$), and entropy change ($\Delta S°$) were determined in order to know the effect of temperature on nickel ions adsorption using SAC and HAC. The value of $\Delta G°$, $\Delta H°$ and $\Delta S°$ can be obtained from [23-~~44~~, 53, 54]:

$$\ln K_e = \frac{\Delta S°}{R} - \frac{\Delta H°}{RT} \quad (10)$$

$$\Delta G° = -RTlnK_e \quad (11)$$

where K_e is the equilibrium constant. The values of $\Delta H°$ (kJ/mol) and $\Delta S°$ (J/molK) can be calculated, respectively from the slope and intercept of $\ln K_e$ versus 1/T plot.

According to *Liu* [53], for an adsorption process described as follows:

$$A + B \leftrightarrows AB \quad (12)$$

where A is the free adsorptive solute molecules, B is the vacant sites on the adsorbent, and AB the occupied sites. The equilibrium constant K_e is defined as K_a and this one is equal to Langmuir constant (K_L) in L/mol, $K_a = K_L(1\ molL^{-1})$ for a diluted solution of adsorbate. K_a is defined as [53]:

$$K_a = \frac{(activity\ of\ accupied\ sites)}{(activity\ of\ vacant\ sites)(activity\ of\ solute\ in\ solution)} = \frac{(AB)}{(B).(A)} \quad (13)$$

Considering that the activity coefficients of the occupied and vacant sites are the same, the Eq. 12 becomes:

$$K_a = \frac{\theta_e}{(1-\theta_e)\gamma_e C_e} \quad (14)$$

were θ_e is the fraction of the surface covered at equilibrium, θ_e = q_e/q_m and γ_e is the activity coefficient of the adsorbate in the solution at equilibrium [53]. Considering a dilute solution ($\gamma_e = 1$) the equilibrium constant could be rewritten as:

$$K_a = \frac{q_e/q_m}{\left(1-q_e/q_m\right)C_e} \quad (15)$$

For a charged adsorbate as Ni(II) ions, the effect of ionic strength was neglected and subsequently the thermodynamic parameters were calculated as an approximation.

In order to evaluate the adsorption mechanism, pseudo-first and pseudo-second order kinetic models were fitted to adsorption kinetic data obtained at 25±1°C. Linearized models can be expressed for the following equations [54]:

$$log(q_e - q_t) = \log q_e - \frac{k_1}{2.303}t \quad (16)$$

$$\frac{t}{q_t} = \frac{1}{k_2 q_e^2} + \frac{1}{q_e}t \quad (17)$$

where k_1 and k_2 are the adsorption rate constants of first and second order kinetic models, in min^{-1} and g/(mg min), respectively; q_e and q_t, in mg/g, are equilibrium adsorption capacity at equilibrium time and at time t. From the slope and the intercept of each linear plot, the adsorption rate constants (k_1 and k_2) can be calculated.

3. Results and Discussion

3.1. Characterization of the adsorbents

Boehm titration tests revealed a low content of acid functional groups on the ACs surface. For SAC the content of carboxyl groups is 0.132 mmol/g, the lactone content is 0.117 mmol/g and the content of phenolic groups is 0.015 mmol/g; for HAC this is 0.019, 0.056 and 0.083 mmol/g, respectively. The pH_{PZC} value, determined by acid–base titration, was found to be 5.2 and 7.1 for SAC and HAC, respectively.

The ACs were characterized by a relatively slight developed porous structure as revealed by N_2 sorption measurements at 77 K (Fig. 1). The textural parameters calculated from the adsorption data are collected in Table 1. The shape of N_2 isotherms indicates the microporous nature of both activated chars (Fig. 1a). The contribution of micropores to the total pore volume is comparable, up to 0.90. SAC exhibits a much more developed porosity compared with HAC. The BET surface area and the micropore volume are 464 vs. 383 m^2/g, and 0.178 vs. 0.151 cm^3/g, respectively. The total pore volume did not exceed 0.2 cm^3/g. The prepared ACs were characterized by a narrow microporosity with an average micropore size in the range of 0.58-0.84 nm. The pore size distribution determined by QSDFT confirmed a pronounced difference between both ACs in the porosity development (Fig. 1b). The SAC sample exhibits an intense maximum at a pore width of 0.57 nm. HAC has significantly wider micropores than SAC. The four maxima are centered at 0.57, 0.72, 1.00 and 1.54 nm.

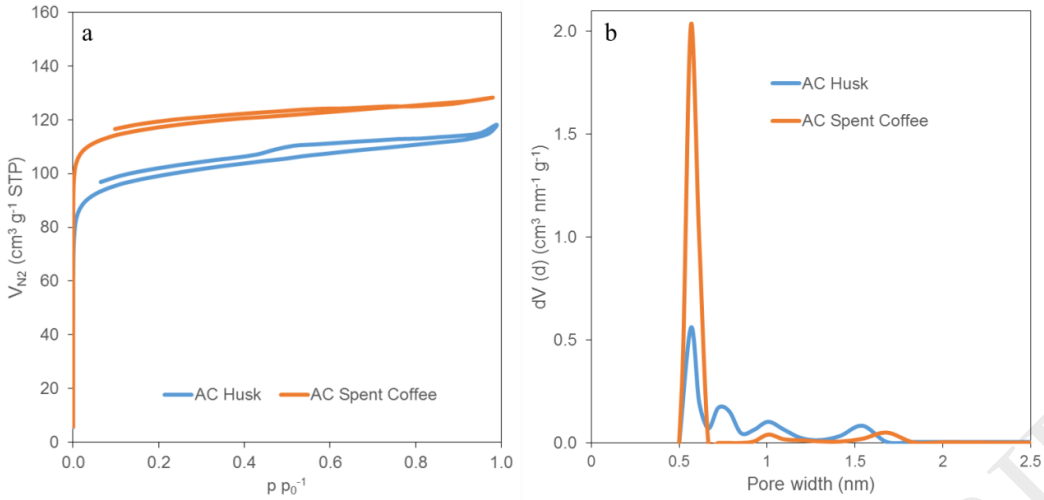

Fig. 1 Nitrogen adsorption-desorption isotherms at 77 K a) and QSDFT pore size distribution b) for activated chars.

Table 1 Textural parameters for SAC and HAC

Sample	S_{BET} m^2/g	V_T cm^3/g	V_{DR} cm^3/g	V_{DR}/V_T	$L_{0,N2}$* nm	$V_{DR,CO2}$ cm^3/g	$S_{0,CO2}$** m^2/g	$L_{0,CO2}$* nm
HAC	383	0.176	0.151	0.86	0.84	0.061	260	0.47
SAC	464	0.197	0.178	0.90	0.58	0.068	216	0.63

* $L_0=10.8/(E_0-11.4)$

** $S_{0,C02}=(2000 \cdot V_{DR,CO2})/L_{0,CO2}$

Because of the narrow porosity, the prepared ACs were analyzed by CO_2 sorption to characterize ultramicropores. Fig. 2 shows the CO_2 adsorption isotherms (a) and the pore size distribution determined by NLDFT (b) in the range of ultramicropores. The textural parameters calculated from the CO_2 isotherm data are also included in Table 1. A bimodal distribution of ultramicropore sizes was revealed for both ACs, showing a maximum at 0.35 nm for both samples and 0.50 and 0.55 nm for SAC and HAC, respectively. The volume and average width of ultramicropores are smaller for HAC compared to SAC. However, the surface area of the narrow micropores is higher for HAC (260 vs. 216 m^2/g).

The measurements of N_2 sorption indicated that it is not possible to obtain the N_2 isotherm for the initial chars because they have a very narrow microporosity, which is not accessible for the nitrogen molecules at 77 K.

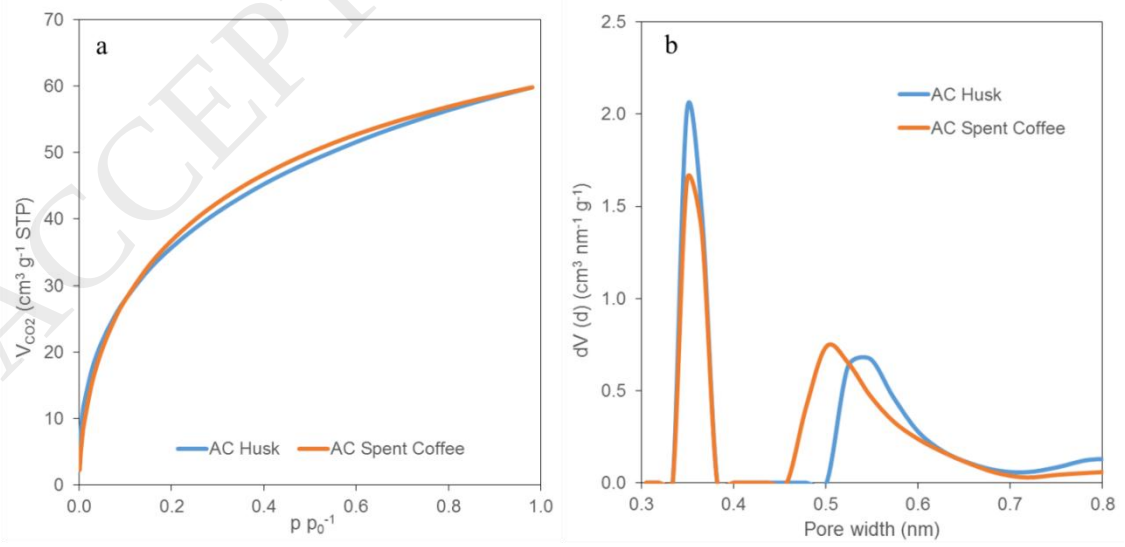

Fig. 2 CO_2 adsorption isotherms at 273 K a) and NLDFT pore size distribution b) for activated chars.

XPS results for C1s core-level spectra of HAC and SAC obtained for the deconvolution of the peaks are shown in Fig 3. Due to the fact that potassium was detected in both samples and overlaps the signal from carbon, the C1s core-level spectra include K $2p_{1/2}$ (~296.3 eV) and K $2p_{3/2}$ (~293.4 eV) deconvoluted peaks, which are associated to the K-O bindings characteristic for K_2O, taking into account the characteristics of the samples. The other five peaks with binding energies of C–C sp^2 at 284.8 eV, C–O (hydroxyl group) at 286.3 eV, C=O (quinone, carbonyl groups) at 287.7 eV, O=C–O (carboxylic groups) at 289 eV and plasmon at 290 eV are found. The distributions of oxygen functional groups in the ACs are summarized in Table 2. The highest contribution of hydroxylic groups was revealed followed by carbonyl and carboxylic groups.

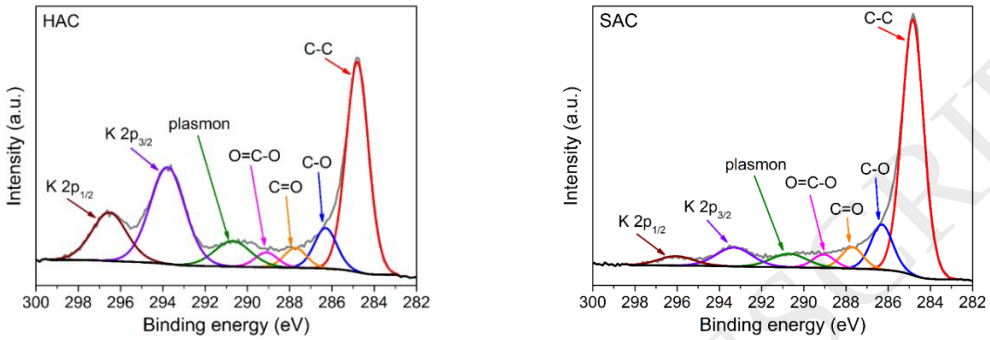

a) b)

Fig. 3 C1s XPS spectrum of a) HAC and b) SAC.

Table 2 Relative content of functional groups obtained from C1s XPS spectrum

Sample	C1s peak deconvolution (%)				
	C-C	C-OH	C=O	O=C-OH	plasmon
HAC	42.5	8.2	4.0	3.0	8.3
SAC	60.9	10.8	5.1	3.3	5.3

Table 3 shows the results of the elemental analysis and surface atomic composition for both ACs. The elemental analysis and XPS results indicate that HAC has more oxygen than SAC. Taking into account the XPS spectra (Fig. 3) the high levels of oxygen for HAC seem to be more related with potassium as K_2O, than with organic funtional groups at the carbon atoms. In general both ACs samples have a low sulphur content, and a lower nitrogen concentration is found for the HAC sample.

Table 3 Elemental composition (on a dry mass basis) for HAC and SAC

Sample	Elemental composition from elemental analysis (wt %)					Surface atomic composition from XPS (at %)			
	C	H	N	S	O	C	N	K	O
HAC	62.0	1.5	1.27	0.4	17.2	66.0	0.8	9.2	24.0
SAC	82.9	1.7	2.57	0.2	8.1	85.4	2.3	2.2	10.1

3.2. The effect of adsorbent doses

Fig. 4 shows the effect of adsorbent doses on the Ni(II) adsorption process for a 100 mL Ni-solution (45 mg Ni/L). From this figure, it can be deduced that the optimal adsorbent doses are 80 mg for SAC and 100 mg for HAC. By further increasing the adsorbent doses, an increase in the equilibrium concentration in the solution can be noticed, and thus a lower adsorption amount on the AC. It is found that at higher adsorbent amounts, particle aggregation occurs, resulting in a decrease of the total free surface area and

an increase of the diffusion path length [8, 55]. This aggregation phenomenon seems to be influenced by the nature of the adsorbent and is faster for SAC than for HAC.

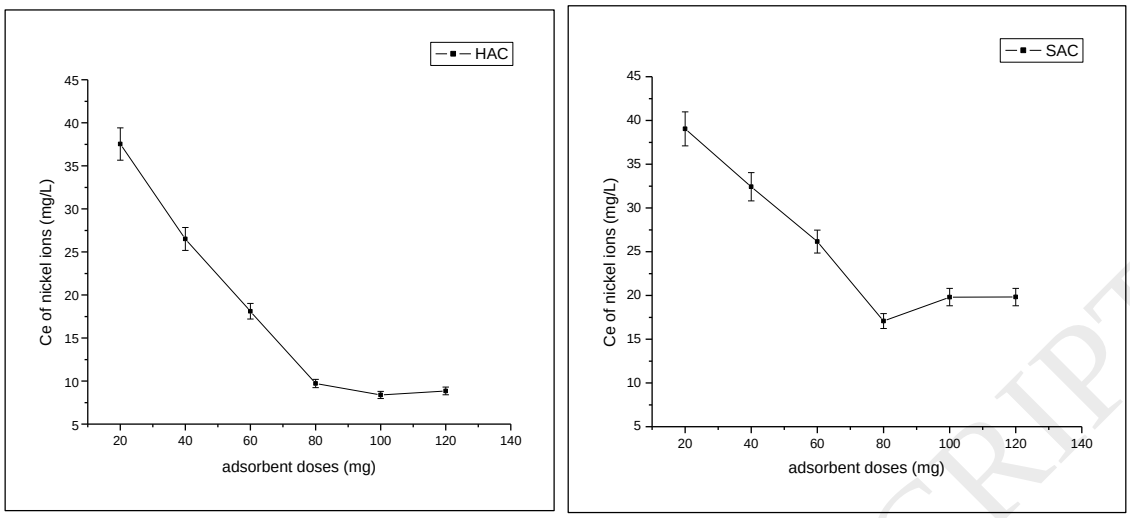

a) b)

Fig. 4 Effect of adsorbent doses a) HAC and b) SAC (C_0 = 45 mg/L, V = 100 mL, pH = 6, T = 25±1 ^{0}C, speed shake 50 rpm, t = 24 h).

3.3. The effect of solution pH

The effect of solution pH on the adsorption process is shown in Fig. 5. A minimum in the Ni(II) equilibrium concentration is obtained when the initial pH is around 6. At low pH, the Ni-ion is not able to replace the bound H^+ or even to enter the AC, as it is positive charged ($pH < pH_{PZC}$). Only when the pH is high enough ($pH > pH_{PZC}$) Ni ions are able to compete with H^+ and to be bound on the functional groups. Additionally, as the AC becomes rather neutral to negative charged, they can enter the AC and its pores, and bind on the active places [56, 57]. Thus, an electrostatic attraction mechanism between the surface and the Ni-ion can take place [58]. At a higher initial pH of 6, the Ni(II) equilibrium concentration in solution increases again, due to the formation of $Ni(OH)^+$, being less competitive in the adsorption process [13]. At an even higher pH than 8, precipitation of $Ni(OH)_2$ starts.

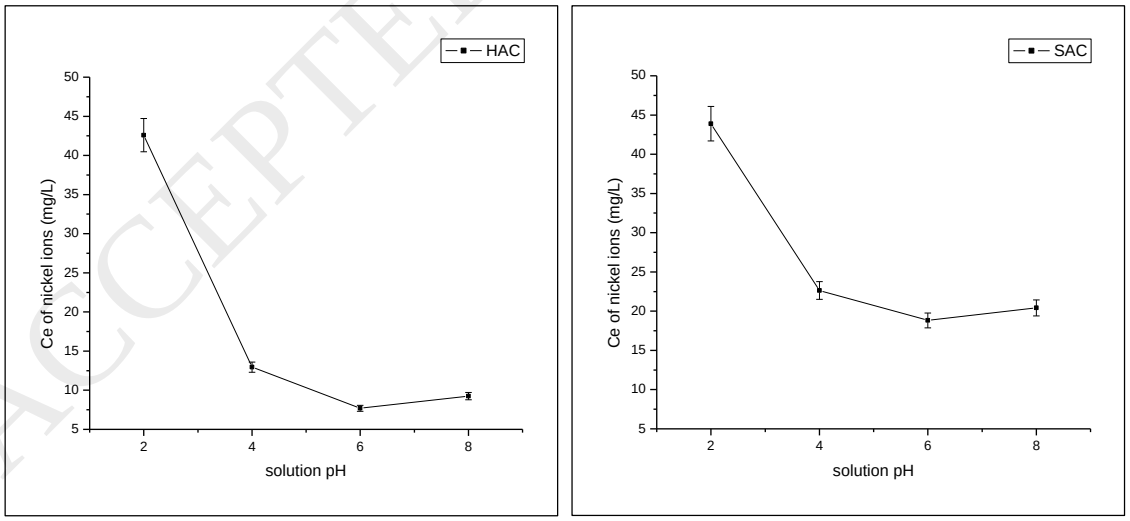

a) b)

Fig. 5 Effect of solution pH a) HAC and b) SAC (C_0 = 45 mg/L, m = 80 mg for SAC and 100 mg for HAC, V = 100 mL, T = 25±1 ^{0}C, shake speed 50 rpm, t = 24 h).

3.4. Adsorption isotherms

In the Fig. 6 the adsorption isotherms are presented at the optimum adsorbent doses and solution pH. The equilibrium adsorption data gave a convex curve. HAC isotherm should be classified as highly affinity, which is indicative of a strong adsorption processes [59]. The adsorption models (Table 4) show a better almost equal fit for the Monolayer Model for Single-Compound Adsorption (MM-SCA) and Langmuir model. From MM-SCA model it is possible to establish that the conditions assumed by Langmuir adsorption theory are not really fulfilled completely. The adsorbed Ni(II) occupies more or less than one ion per site of adsorption. For the HAC the number of ions per site *n* are in the range of 1-2, pointing more to a multi-ion adsorption process and Ni ions could be binding either by one ion per site or two ions per site. For the SAC the opposite occurs (n<1), in this case the Ni ions might be adsorbed at more than one binding site (multi-anchorage adsorption mechanism). These results not only indicate a difference in characteristics of both AC but also suggest a difference in the adsorption mechanism. The density of receptor sites (N_m) is greater for SAC than for HAC. This suggests that the multi-ion adsorption of Ni onto HAC could decrease the binding ability of neighbour receptor sites. The multi-ion adsorption mechanism on HAC could be related with the oxygen content. But this is not only determined to the organic oxygen functionalities (ATR-FTIR results) but also associated to the mineral matter as K_2O (Table 3), being much higher for HAC than for SAC. Thus caution is at his place. Additionally, the monolayer adsorbed quantity (Q_0) has almost the same value for both adsorbents, which is not in agreement with adsorption isotherms (Fig. 6) where HAC adsorbs higher amounts than SAC at each initial Ni(II) concentration as calculated by the Langmuir model. Taking into account these observations and the small difference in the correlation coefficient (R^2) for both models, the Langmuir model seems to be more appropriated for the equilibrium description. From Langmuir model the separation factor (R_L) is in the range of 0-1, indicating a favourable adsorption process for nickel ions, as both R^2 have acceptable values. The maximum adsorption capacity for HAC is larger than for SAC. The mean energy of sorption per mole of adsorbate (*E*) is for both less than 8 kJ/mol, corresponding rather with a physical adsorption process, even by taking the unfavourable fit of D-R model into account.

The removal percentage for the initial concentration of nickel ions within 30-120 mg/L is in the range of 29.1-65.2% for SAC and 44.6-90.8% for HAC. It was found for HAC that at initial concentration below 20 mg/L of Ni(II), a complete removal was noticed. In the case of SAC, an almost 100% removal below 10 mg/L of Ni(II) was measured. This is the reason why removal studies were examined in the range of 30-120 mg/L Ni(II). In all cases, HAC performs better and has a higher removal %. Table 5 gives a literature survey of several adsorbents with their maximum sorption capacity for Ni(II). It can be noticed that HAC and SAC can compete with the literature results. Additionally, both surface area and the pore size of the AC do not seem to be the determining factor in the adsorption process. Both AC types are microporous in nature and SAC has a greater specific surface area (Table 1). In contrast, the higher amount of oxygen present in HAC (Table 3) is more favourable towards the Ni-ion adsorption process and mechanism. After adsorption a high increment of potassium was found in the solution, 12.1 and 12.6 mg/L for SAC and HAC, respectively, indicating an ion exchange process between the potassium-ion and the Ni(II) present in the solution.

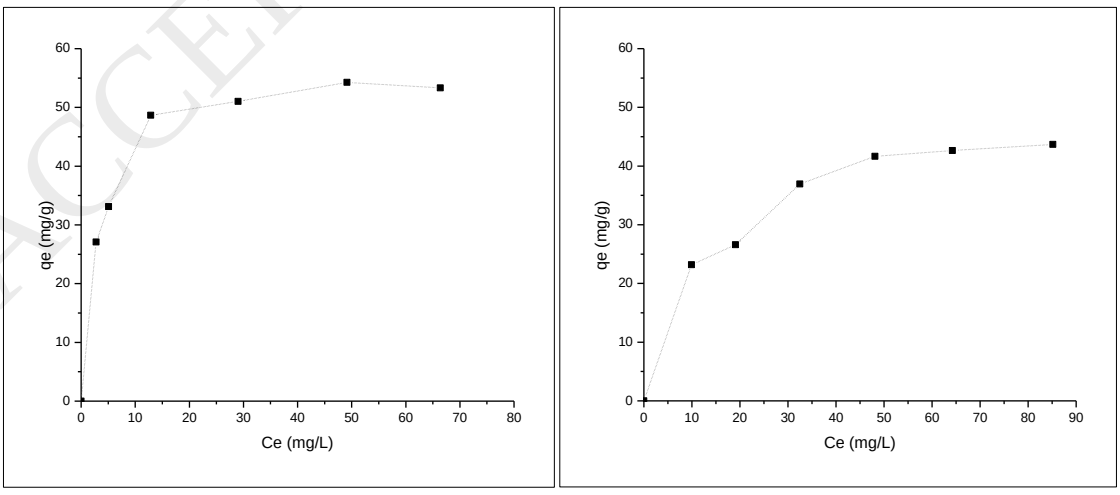

a) b)

Fig. 6 Adsorption isotherms a) HAC, b) SAC (C_0 = 30-120 mg/L, m = 80 mg for SAC and 100 mg for HAC, V = 100 mL, pH = 6, T = 25±1 °C, shake speed 50 rpm, t = 24 h).

Table 4 Isotherm constants for nickel (II) adsorption onto SAC and HAC

Isotherm model	Parameters	Type of adsorbent	
		SAC	HAC
Langmuir	q_m (mg/g)	51.94	57.14
	K_L (L/mg)	0.071	0.315
	R_L	(0.105-0.331)	(0.026-0.096)
	R^2	0.9553	0.9778
Freundlich	K_F	10.95	23.64
	$1/n$	0.33	0.22
	R^2	0.9406	0.8907
D-R	q_s (mg/g)	40.49	50.77
	K_D (mol^2/J^2)	1E-05	1E-06
	E (kJ/mol)	0.223	0.707
	R^2	0.7811	0.8841
MM-SCA	Q_0 (mg/g)	55.17	55.82
	N_m	62.69	48.75
	n	0.88	1.14
	R^2	0.9567	0.9801

Table 5 Adsorption capacities of different adsorbents for nickel ions removal from aqueous solutions

Adsorbent	Maximum adsorption capacity by Langmuir model, q_m (mg/g)	Solution pH	Dosage (g/L)	Concentration range (mg/L)	Reference
Urea-modified activated carbon derived from Pennisetum alopecuroides, PUAC-4	29.5	7	0.6	10-30	[6]
Almond husk activated carbon	18.84	5	5	25-250	[61]
Amine-modified Fireweed activated carbon, AFWC	10.12	5	0.8	1-40	[62]
Commercially powdered activated carbon, PAC	2.29	5	0.8	1-40	[62]
Activated carbon residue from biomass gasification, ACR	62.9	8	5	25-125	[63]
Activated carbon from doum seed (Hyphaenethebaica) coat, DACI	4.93	7	10	10-40	[8]
Activated carbon from doum seed (Hyphaenethebaica) coat, DACII	13.51	7	10	10-40	[8]
Multi-walled carbon nanotubes	18.08	6	10	10-200	[64]
Multi-walled oxidized carbon nanotubes	49.26	6	10	10-200	[64]
Activated carbon from coffee husk, HAC	57.14	6	1	30-120	Present study
Activated carbon from spent coffee, SAC	51.91	6	0.8	30-120	Present study

ATR-FTIR spectra (Supplementary material) of ACs before and after adsorption reveal that for HAC the bands located at 1440, 1364, 698 and 626 cm^{-1} corresponding with O–H, in and out of plane bending vibrations tending to be less pronounced after the adsorption process, denoting the interaction of Ni ions with these functionalities. For SAC, the spectra before and after adsorption test have similar

characteristics, the bands located at 1725 cm^{-1} (stretching vibrations of carbonyl/carboxylic groups on the edges of layer planes), 628-872 cm^{-1} (O–H out of plane bending) do not play a significant role during Ni removal.

3.5. Desorption tests and reusability of activated carbons

Fig. 7 depicts the removal and desorption effectiveness during 3 cycles of adsorption-desorption test. It is observed that HAC has better removal and desorption effectiveness than SAC in all cycles, confirming the active role of O–H functionalities during the adsorption. The H^+ ions replace the Ni-ions bonded to the oxygen functionalities, recovering almost during the first two cycles HAC the total adsorption capacity.

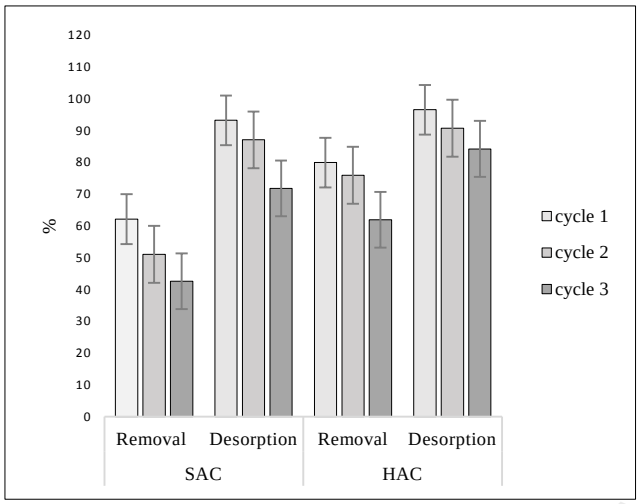

Fig. 7 Adsorption-desorption cycles (C_0 = 45 mg/L, m = 80 mg for SAC and 100 mg for HAC, V = 100 mL, T = 25±1 ^{0}C, shake speed 50 rpm, t = 24 h).

3.6. Adsorption kinetics

The kinetic results for Ni(II) show a fast adsorption process: the equilibrium is reached in less than 2 h (Fig. 8). For the pseudo-first-order model a low regression coefficient (R^2) is found, only 0.5. For the pseudo-second order model, R^2 is much better (0.9889 and 0.9602 for HAC and SAC, respectively). The adsorption process described by the pseudo-second order model assumes that the rate-limiting step may be chemisorption promoted either by valence forces, through sharing electrons between adsorbent and nickel ions, or by covalent forces, through exchange of electrons [65].

With the regression equations obtained for the pseudo-second order models, the rate constants (k_2), 0.0016 and 0.0014 $g/mg\ min$ for HAC and SAC were obtained, respectively. HAC adsorbs Ni(II) faster than SAC, and its maximum amount of adsorbed Ni(II) is higher.

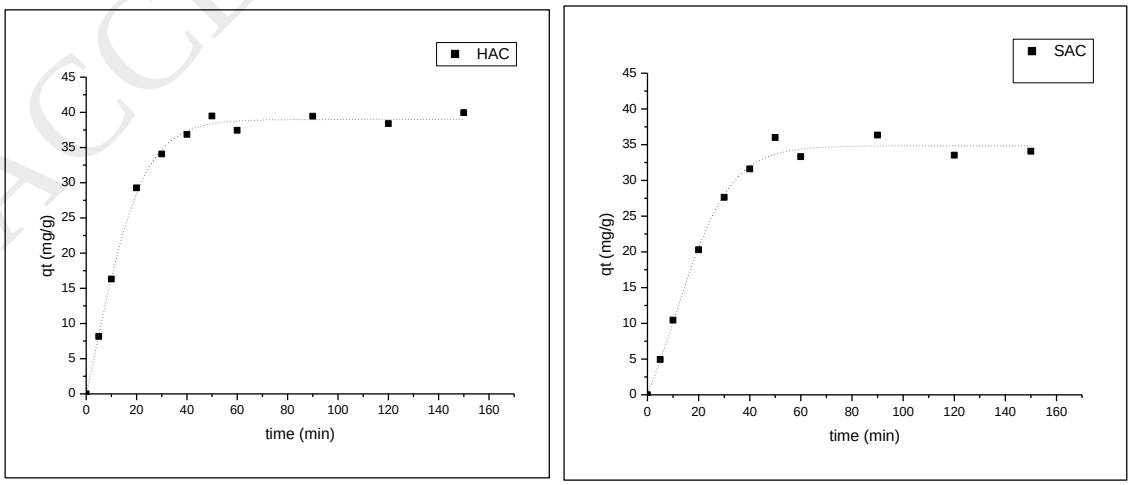

a) b)

Fig. 8 Kinetic results for Ni(II) a) HAC, b) SAC (C_0 = 45 mg/L, m = 80 mg for SAC and 100 mg for HAC, V = 100 mL, pH = 6, T = 25±1 ^{0}C, shake speed 50 rpm). The drawn line is a based on Langmuir trend line.

3.7. Adsorption thermodynamics

The relationship between temperature and removal of nickel ions is given in Fig. 9 (a and b). The results evidence an increment in removal when temperature was increased from 298 K to 328 K for both adsorbents. At very low concentration of Ni ions (30 mg/L) and higher temperatures (308-328 K), HAC removal is >94%, which in view of practical application, i.e. reaching the safety norm, is quite interesting. The temperature affects the equilibrium of adsorption; higher temperatures tend to improve the ability of adsorption and facilitates diffusion in the pores of the adsorbent materials [13, 66].

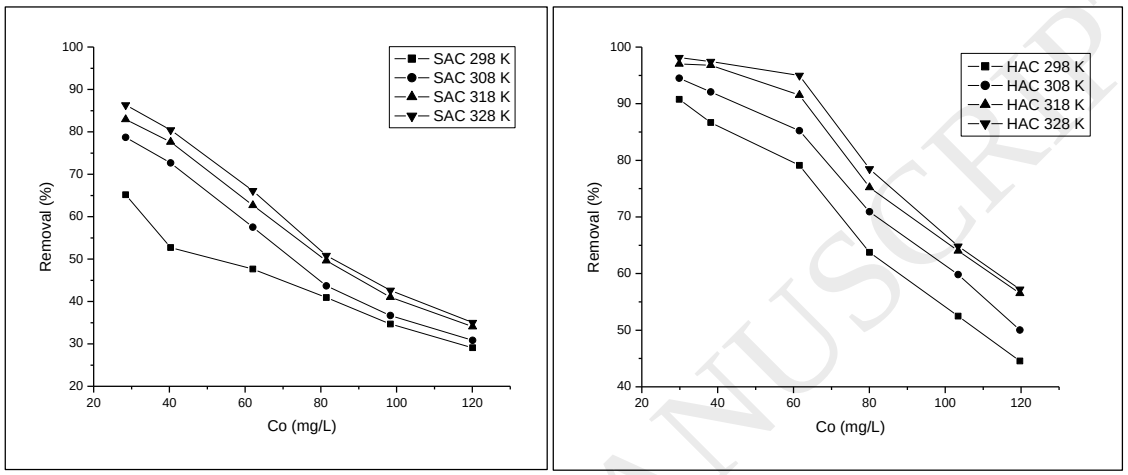

a) b)

Fig. 9 Effect of temperature on nickel (II) removal a) SAC, b) HAC (C_0 = 45 mgL^{-1}, m = 80 mg for SAC and 100 mg for HAC, V = 100 mL, pH = 6, t = 24 h, shake speed = 50 rpm).

The approximate thermodynamic parameters are shown in Table 6, according Eqs. 4 and 15. The values of K_L for SAC and HAC are however in L/mg (0.071 and 0.315, Table 4 for 298K~~)~~) so for using K_L as K_e they have to be converted in L/mol= K_L*molecular weight of Ni*1000 (according ref. 53), resulting into 4168 and 18 473 L/mol for SAC and HAC respectively. For all other temperatures the same strategy is applied, according Eq. 11 resulting in the ΔG° values listed in Table 6. According Eq. 10, ΔH° and ΔS° can be obtained and are given in Table 6. The negative ΔG° and positive ΔH° for both approaches are of the same magnitude and suggest that the adsorption process of nickel ions on SAC and HAC is spontaneous but endothermic in nature. The ΔG° becomes gradually more negative when temperature increased from 298 to 328 K, which suggests that adsorption process is more favourable at higher temperature. The ΔH° value for ACs is greater than 20 kJ/mol**,** rather pointing to a more chemical bounding process [53]. This is not really in conflict with the results obtained by the D-R fit, suggesting the implication of physical and chemical processes during the adsorption. Even when the equilibrium constants K_a (Eq. 15) and K_L (Eq. 4) have the same interpretation as discussed by *Liu* [53], better fits of Eq. 10 are achieved using K_a (Eq. 15) as equilibrium constant.

Table 6 Thermodynamic parameters for nickel (II) ions.

		R^2 (Eq. 9)	ΔH° (kJ/mol)	ΔS° (J/mol.K)	ΔG° (kJ/mol)			
					298 *K*	308 *K*	318 *K*	328 *K*
Based in K_L (Eq. 4)	SAC	0.7606	39.07	202.8	-20.65	-24.52	-25.51	-26.98
	HAC	0.9844	40.95	218.7	-24.34	-26.14	-28.81	-30.75
Based in K_a (Eq. 14)	SAC	0.9766	56.27	256.3	-19.96	-21.94	-24.12	-24.93
	HAC	0.9902	43.91	228.2	-24.27	-25.30	-26.88	-28.21

4. Conclusions

Spent coffee and coffee husk activated carbon (SAC and HAC) show a high affinity for Ni(II) adsorption. The best adsorbent doses were 80 mg and 100 mg for SAC and HAC, respectively, at an optimal pH around 6. The adsorption capacity for HAC was higher than for SAC. At low initial concentration of nickel (30 mg/L) and higher temperatures (308-328 K), the removal is almost complete for HAC. The Monolayer Model for Single-Compound Adsorption and Langmuir model fitted better the adsorption data. However, Langmuir model seems to be more appropriated for equilibrium description. The adsorbed Ni(II) occupies more or less than one ion per site of adsorption. For HAC a multi-ion adsorption process occurs, meanwhile for SAC Ni ions might be adsorbed at more than one binding site (multi-ion anchorage adsorption mechanism). The surface area and the pore size of the ACs do not seem to be the determining factor in the adsorption process. These ACs are microporous in nature. The higher amount of oxygen associated to the mineral matter as K_2O and carbon functionalities corresponding with O–H present in HAC seems to be more in favour towards the Ni-ion adsorption process and multi-ion anchorage mechanism. Thermodynamic parameters show an endothermic adsorption process, which is more favourable with increasing temperature. Adsorption kinetics demonstrate a quick process, which can be described by a pseudo-second order kinetic model. HAC and SAC could be suitable adsorbents in the removal of Ni(II) from aqueous solution. It is observed that HAC has better removal and desorption effectiveness than SAC.

Author contribution: Mónica Hernández Rodríguez performed, conceived and designed the experiments and wrote the paper; Jan Yperman and Robert Carleer designed the experiments, analysed the data and wrote the paper; Jens Maggen performed and designed the elemental experiments, performed and designed the pyrolysis and activation experiments; Dessalegn Daddi performed pyrolysis experiment; Grazyna Gryglewicz performed and analysed the N_2 adsorption and XPS experiments and wrote the paper; Bart Van der Bruggen, José Falcón Hernández and Alexis Otero Calvis wrote the paper.

The authors declare no conflict of interest

References

[1] J.M. Dias, M.C.M. Alvim-Ferraz, M.F. Almeida, J. Rivera-Utrilla, M. Sánchez-Polo, Waste materials for activated carbon preparation and its use in aqueous-phase treatment: A review, J. Environ. Manage. 85 (2007) 833–846.

[2] A. Ahmadpour, M. Tahmasbi, T. Rohani Bastami, J. Amel Besharati, Rapid removal of cobalt ion from aqueous solutions by almond green hull, J. Hazard. Mater. 166 (2009) 925–930.

[3] F. Fu, Q. Wang, Removal of heavy metal ions from wastewaters: A review, J. Environ. Manage. 92 (2011) 407 – 418.

[4] D. Sud, G. Mahajan, M.P. Kaur, Agricultural waste material as potential adsorbent for sequestering heavy metal ions from aqueous solutions – A review, Bioresour. Technol. 99 (2008) 6017–6027.

[5] M. Karnib, A. Kabbani, H. Holail, Z. Olama, Heavy Metals Removal Using Activated Carbon, Silica and Silica Activated Carbon Composite, Energy Procedia 50 (2014) 113 – 120.

[6] Y. Kang, Z. Guo, J. Zhang, H. Xie, H. Liu, C. Zhang, Enhancement of Ni (II) removal by urea-modified activated carbon derived from Pennisetum alopecuroides with phosphoric acid activation, J. Taiwan Inst. Chem. Eng. 000 (2015) 1–7.

[7] T. Maneerung, J. Liew, Y. Dai, S. Kawi, C. Chong, C-H. Wang, Activated carbon derived from carbon residue from biomass gasification and its application for dye adsorption: Kinetics, isotherms and thermodynamic studies, Bioresour. Technol. 200 (2016) 350–359.

[8] M. El-Sadaawy, O. Abdelwahab, Adsorptive removal of nickel from aqueous solutions by activated carbons from doum seed (Hyphaenethebaica) coat, Alexandria Eng. J. (2014) xxx, xxx–xxx.

[9] M. Nadeem, A. Mahmood, S.A. Shahid, S.S. Shah, A.M. Khalid, G. McKay, Sorption of lead from aqueous solution by chemically modified carbon adsorbents, J. Hazard. Mater. 138 (2006) 604–613.

[10] F.-S. Zhang, J.O. Nriagu, H. Itoh, Mercury removal from water using activated carbons derived from organic sewage sludge, Water Res. 39 (2005) 389–395.

[11] A.M. Youssef, T. El-Nabarawy, S.E. Samra, Sorption properties of chemically-activated carbons: 1. Sorption of cadmium (II) ions. Colloids Surf. A Physicochem. Eng. Asp. 235 (2004) 153–163.

[12] H.Yanagisawa, Y. Matsumoto, M. Machida, Adsorption of Zn(II) and Cd(II) ions onto magnesium and activated carbon composite in aqueous solution, Appl. Surf. Sci. 256 (2010) 1619 - 1623.

[13] M. Ghasemi, M.Z. Khosroshahy, A.B. Abbasabadi, N. Ghasemi, H. Javadian, M. Fattahi, Microwave-assisted functionalization of Rosa Canina-L fruits activated carbon with tetraethylenepentamine and its

adsorption behaviour toward Ni (II) in aqueous solution: Kinetic, equilibrium and thermodynamic studies, Powder Technol. 274 (2015) 362–371.

[14] A. Üçer, A. Uyanik, S.F. Aygün, Adsorption of Cu(II), Cd(II), Zn(II), Mn(II) and Fe(III) ions by tannic acid immobilised activated carbon, Sep. Purif. Technol. 47 (2006) 113 - 118.

[15] H.G. Park, T.W. Kim, M.Y. Chae, I.K. Yoo, Activated carbon-containing alginate adsorbent for the simultaneous removal of heavy metals and toxic organics, Process Biochem. 42 (2007) 1371 – 1377.

[16] C.K. Ahn, D. Park, S.H. Woo, J.M. Park, Removal of cationic heavy metal from aqueous solution by activated carbon impregnated with anionic surfactants, J. Hazard. Mater. 164 (2009) 1130 - 1136.

[17] M. Ahmedna, W.E. Marshall, R.M. Rao, Production of granular activated carbons from select agricultural by-products and evaluation of their physical, chemical and adsorption properties, Bioresour. Technol. 71 (2000) 113–123.

[18] U. Kumar, Agricultural products and by-products as a low cost adsorbent for heavy metal removal from water and wastewater: A review, Sci. Res. Essays 1 (2006) 033-037.

[19] L.C.A. Oliveira, E. Pereira, I.R. Guimaraes, A. Vallone, M. Pereira, J.P. Mesquita, K. Sapag, Preparation of activated carbons from coffee husks utilizing $FeCl_3$ and $ZnCl_2$ as activating agents, J. Hazard. Mater. 165 (2009) 87–94.

[20] M. Gonçalves, M.C. Guerreiro, L.C.A. Oliveira, C. Solar, M. Nazarro, K. Sapag, Micro Mesoporous Activated Carbon from Coffee Husk as Biomass Waste for Environmental Applications, Waste Biomass Valor 4 (2013) 395–400.

[21] S. Rovani, A. G. Rodrigues, L. F. Medeiros, R. Cataluña, É. C. Lima, A. N. Fernandes, Synthesis and characterisation of activated carbon from agroindustrial waste—Preliminary study of 17 β -estradiol removal from aqueous solution, J. of Environ. Chem. Eng. 4 (2016) 2128–2137.

[22] J.M. Dias, M.C.M. Alvim-Ferraz, M.F. Almeida, J. Rivera-Utrilla, M. Sánchez-Polo, Waste materials for activated carbon preparation and its use in aqueous-phase treatment: A review, J. Environ. Manage. 85 (2007) 833–846.

[23] M.A. Ahmad, N.K. Rahman, Equilibrium, kinetics and thermodynamic of Remazol Brilliant Orange 3R dye adsorption on coffee husk-based activated carbon. Chem. Eng. J. 170 (2011) 154–161.

[24] V. Boonamnuayvitaya, S. Sae-ung, W. Tanthapanichakoon, Preparation of activated carbons from coffee residue for the adsorption of formaldehyde. Sep. and Purif. Technol. 42 (2005) 159–168.

[25] C. Djilani, R. Zaghdoudi, A. Modarressi, M. Rogalski, F. Djazi, A. Lallam, Elimination of organic micropollutants by adsorption on activated carbon prepared from agricultural waste. Chem. Eng. J. 189–190 (2012) 203–212.

[26] K. Kante, C. Nieto-Delgado, J.R. Rangel-Mendez, T.J. Bandosz, Spent coffee-based activated carbon: Specific surface features and their importance for H2S separation process. J. Hazard. Mater. 201–202 (2012) 141–147.

[27] L. Khenniche, F. Benissad-Aissani, Adsorptive Removal of Phenol by Coffee Residue Activated Carbon and Commercial Activated Carbon: Equilibrium, Kinetics, and Thermodynamics. J. Chem. Eng. Data 2010, 55, 4677–4686.

[28] X. Ma, F. Ouyang, Adsorption properties of biomass-based activated carbon prepared with spent coffee grounds and pomelo skin by phosphoric acid activation. Appl. Surf. Sci. 268 (2013) 566–570.

[29] S.L. Ching, M.S. Yusoff, H.A. Aziz, M. Umar, Influence of impregnation ratio on coffee ground activated carbon as landfill leachate adsorbent for removal of total iron and orthophosphate. Desalination 279 (2011) 225–234.

[30] F. Boudrahem, F. Aissani-Benissad, H. Ait-Amar, Batch sorption dynamics and equilibrium for the removal of lead ions from aqueous phase using activated carbon developed from coffee residue activated with zinc chloride. J. Environ. Manage. 90 (2009) 3031–3039.

[31] F. Boudrahem, A. Soualah, F. Aissani-Benissad, Pb(II) and Cd(II) Removal from Aqueous Solutions Using Activated Carbon Developed from Coffee Residue Activated with Phosphoric Acid and Zinc Chloride. J. Chem. Eng. Data 56 (2011) 1946–1955.

[32] WHO, Guidelines for drinking-water quality. In: Chemical Fact Sheets. World Health Organization, Geneva 2004.

[33] WHO, Guidelines for drinking-water quality, 1st Addedum. In: Chemical Fact Sheets. World Health Organization, Geneva 2006.

[34] T. Cornelissen, J. Yperman, G. Reggers, S. Schreurs and R. Carleer. Flash co-pyrolysis of biomass with polylactic acid. Part I: influence on bio-oil yield and heating value. Fuel 87 (2008) 1031-1041.

[35] P.C.C. Faria, J.J.M. Orfao, M.F.R. Pereira, Adsorption of anionic and cationic dyes on activated carbons with different surface chemistries, Water Res. 38 (2004) 2043–2052.

[36] N. Wibowo, L. Setyadhi, D. Wibowo, J. Setiawan, S. Ismadji, Adsorption of benzene and toluene from aqueous solutions onto activated carbon and its acid and heat treated forms: Influence of surface chemistry on adsorption, J. Hazard. Mater. 146 (2007) 237–242.

[37] F. Adib, A. Bagreev, T.J. Bandosz, Effect of pH and surface chemistry on the mechanism of H_2S removal by activated carbons, J. Colloid Interface Sci. 216 (1999) 360–369.

[38] H.P. Boehm, Chemical identification of surface groups. In: Eley DD, Herman Pines, Paul B Weisz, editors. Adv Catal. Academic Press; 1966. p. 179–274.
[39] H.P. Boehm, Some aspects of the surface-chemistry of carbon-blacks and other carbons, Carbon 32 (1994) 759–769.
[40] F. Stoeckil, E. Daguerre, A. Guillot, The development of micropore volumes and widths during physical activation of various precursors, Carbon 37 (1999) 2075-2077.
[41] A.V. Neimark, Y. Lin, P.I. Ravikovitch, M. Thommes, Quenched solid density functional theory and pore size analysis of micro-mesoporous carbons, Carbon 47 (2009) 1617-1628.
[42] F. Stoeckli, M.V. Lopez-Ramon, C. Moreno-Castilla, Adsorption of phenolic compounds from aqueous solutions, by activated carbons, described by the Dubinin−Astakhov equation, Langmuir 17 (2001) 3301-3306.
[43] P. Tarazona, U. Marini Bettolo Marconi, R. Evans, Phase equilibria of fluid interfaces and confined fluids: non-local versus local density functionals, Mol. Phys. 60 (1987) 573.
[44] W.E. Oliveira, A. S. Franca, L.S. Oliveira, S.D. Rocha, Untreated coffee husks as biosorbents for the removal of heavy metals from aqueous solutions, J. Hazard. Mater. 152 (2008) 1073–1081.
[45] K.Y. Foo, B.H. Hameed, Insights into the modeling of adsorption isotherm systems, Chem. Eng. J. 156 (2010) 2–10.
[46] S. Kundu, A.K. Gupta, Arsenic adsorption onto iron oxide-coated cement (IOCC): regression analysis of equilibrium data with several isotherm models and their optimization, Chem. Eng. J. 122 (2006) 93–106.
[47] A.B. Pérez-Marín, V. Meseguer Zapata, J.F. Ortuno, M. Aguilar, J. Sáez, M. Llorens, Removal of cadmium from aqueous solutions by adsorption onto orange waste, J. Hazard. Mater. B139 (2007) 122–131.
[48] K.R. Hall, L.C. Eagleton, A. Acrivos, T. Vermeule, Pore and solid-diffusion kinetics in fixed-bed adsorption under constant-pattern conditions, Ind. Eng. Chem. Fund. 5 (1966) 212–223.
[49] L. Sellaoui, M. Bouzid, L. Duclaux, L. Reinert, S. Knani, A. Ben Lamine, Binary adsorption isotherms of two ionic liquids and ibuprofen on an activated carbon cloth: simulation and interpretations using statistical and COSMO- RS models. R. Soc. Chem. Adv. 6 (2016) 67701–67714.
[50] L. Sellaoui, G.L. Dotto, A. Ben Lamine, A. Erto, Interpretation of single and competitive adsorption of cadmium and zinc on activated carbon using monolayer and exclusive extended monolayer models. Environ. Sci. Pollut. Res. 24 (2017) 19902-19908.
[51] M.M. Dubinin, The potential theory of adsorption of gases and vapors for adsorbents with energetically non-uniform surface, Chem. Rev. 60 (1960) 235–266.
[52] Mobasherpour, E. Salahi, M. Pazouki, Removal of nickel (II) from aqueous solutions by using nano-crystalline calcium hydroxyapatite, J. Saudi Chem. Soc. 15 (2011) 105–112.
[53] Yu Liu, Is the Free Energy Change of Adsorption Correctly Calculated?, J. Chem. Eng. Data 54 (2009) 1981–1985.
[54] M.A. Tofighy, T. Mohammadi, Adsorption of divalent heavy metal ions from water using carbon nanotube sheets, J. Hazard. Mater. 185 (2011) 140–147.
[55] L.S. Oliveira, A.S. Franca, T.M. Alves, S.D.F. Rocha, Evaluation of untreated coffee husks as potential biosorbents for treatment of dye contaminated waters, J. Hazard. Mater. 155 (2008) 507–512.
[56] S.A. Kosa, Gh. Al-Zhrani, M. Abdel Salam, Removal of heavy metals from aqueous solutions by multi-walled carbon nanotubes modified with 8-hydroxyquinoline, Chem. Eng. J. 181–182 (2012) 159–168.
[57] W.F. Chen, R. Parette, J.Y. Zou, F.S. Cannon, Arsenic removal by iron-modified activated carbon, Water Res. 41 (2007) 1851–1858.
[58] W.-F. Chen, L. Pan, L.-F. Chen, Z. Yu, Q. Wang, C.-C. Yan, Comparison of EDTA and SDS as potential surface impregnation agents for lead adsorption by activated carbon, Appl. Surf. Sci. 309 (2014) 38–45. 48
[59] D. Myers, Surfaces, Interfaces, and Colloids: Principles and Applications, Second Edition, 1999.
[60] L. Sellaoui, H. Guedidi, S. Knani, L. Reinert, L. Duclaux, A.B. Lamine, Application of statistical physics formalism to the modeling of adsorption isotherms of ibuprofen on activated carbon. Fluid Ph. Equilibria 387 (2015) 103–110.
[61] H. Hasar, Adsorption of nickel(II) from aqueous solution onto activated carbon prepared from almond husk, J. Hazard. Mater. 97 (2003) 49–57.
[62] A.D. Dwivedi, S.P. Dubey, M. Sillanpää, Y.-N. Kwon, C. Lee, Distinct adsorption enhancement of bi-component metals (cobalt and nickel) by Fireweed-derived carbon compared to activated carbon: Incorporation of surface group distributions for increased efficiency, Chem. Eng. J. 281 (2015) 713–723.
[63] H. Runtti, S. Tuomikoski, T. Kangas, U. Lassi, T. Kuokkanen, J. Rämö, Chemically activated carbon residue from biomass gasification as a sorbent for iron (II), copper (II) and nickel (II) ions, J. Water Process Eng. 4 (2014) 12–24.
[64] M.I. Kandah, J.-L. Meunier, Removal of nickel ions from water by multi-walled carbon nanotubes, J. Hazard. Mater. 146 (2007) 283–288.
[65] Y.S. Ho, G. McKay, The kinetics of sorption of divalent metal ions onto sphagnum moss peat, Water Res. 34 (2000) 735–742.
[66] J. Lin, Y. Zhan, Z. Zhu, Adsorption characteristics of copper (II) ions from aqueous solution onto humic acid-immobilized surfactant-modified zeolite, Colloids Surf. A Physicochem. Eng. Asp. 384 (2011) 9–16.

.